Diagnosing the nature of the 126 GeV 'Higgs' signal

Jack Gunion
U.C. Davis

CERN, BSM lunch/forum, January 24, 2013

Higgs couplings Collaborators: Belanger, Beranger, Ellwanger, Kraml

1. *"Higgs Couplings at the End of 2012"* G. Belanger, B. Dumont, U. Ellwanger, J. F. Gunion and S. Kraml. arXiv:1212.5244 [hep-ph]

NMSSM Collaborators: G. Belanger, U. Ellwanger, Y. Jiang, S. Kraml, J. Schwarz

1. *"Higgs Bosons at 98 and 125 GeV at LEP and the LHC"* G. Belanger, U. Ellwanger, J. F. Gunion, Y. Jiang, S. Kraml and J. H. Schwarz. arXiv:1210.1976 [hep-ph]
2. *"Two Higgs Bosons at the Tevatron and the LHC?"* G. Belanger, U. Ellwanger, J. F. Gunion, Y. Jiang and S. Kraml. arXiv:1208.4952 [hep-ph]
3. *"Diagnosing Degenerate Higgs Bosons at 125 GeV"* J. F. Gunion, Y. Jiang and S. Kraml. arXiv:1208.1817 [hep-ph]
4. *"Could two NMSSM Higgs bosons be present near 125 GeV?"* J. F. Gunion, Y. Jiang and S. Kraml. arXiv:1207.1545 [hep-ph]
5. *"The Constrained NMSSM and Higgs near 125 GeV"* J. F. Gunion, Y. Jiang and S. Kraml. arXiv:1201.0982 [hep-ph] Phys. Lett. B **710**, 454 (2012)

2HDM Collaborators: Alexandra Drozd, Bohdan Grzadkowski, Yun Jiang

1. *"Two-Higgs-Doublet Models and Enhanced Rates for a 125 GeV Higgs"* A. Drozd, B. Grzadkowski, J. F. Gunion and Y. Jiang. arXiv:1211.3580 [hep-ph]

Higgs-like LHC Excesses at $125 - 126$ GeV

- **Experimental Higgs-like excesses: define**

$$R_Y^h(X) = \frac{\sigma(pp \to Y \to h)\mathrm{BR}(h \to X)}{\sigma(pp \to Y \to h_{SM})\mathrm{BR}(h_{SM} \to X)}\,, \quad R^h(X) = \sum_Y R_Y^h\,, \qquad (1)$$

where $Y = gg$, VV, Vh or $t\bar{t}h$. The notation $\mu \equiv R$ is sometimes employed.

Experimental results are now available for many channels, where the experimental channel is usually a mixture of the theoretical channels.

$$\mu_k = \sum T_k^i \widehat{\mu}_i \qquad (2)$$

where the T_k^i give the amount of contribution to the experimental channel k coming from the theoretically defined channel i and $\widehat{\mu}_i$ is the prediction for a given theoretical channel. The observed μ_k values and T_k^i values are summarized in the following tables.

Channel	Signal strength μ	m_H (GeV)	Production mode			
			ggF	VBF	VH	ttH
$H \to \gamma\gamma$ (4.8 fb^{-1} at 7 TeV + 13.0 fb^{-1} at 8 TeV) [?]						
$\mu(\mathrm{ggF} + \mathrm{ttH}, \gamma\gamma)$	1.85 ± 0.52	126.6	100%	–	–	–
$\mu(\mathrm{VBF} + \mathrm{VH}, \gamma\gamma)$	2.01 ± 1.23	126.6	–	60%	40%	–
$H \to ZZ$ (4.6 fb^{-1} at 7 TeV + 13.0 fb^{-1} at 8 TeV) [?, ?]						
Inclusive	$1.01^{+0.45}_{-0.40} \to 0.97^{+0.45}_{-0.40}$	125	87%	7%	5%	1%
$H \to WW$ (13.0 fb^{-1} at 8 TeV) [?, ?]						
$e\nu\mu\nu$	$1.42^{+0.58}_{-0.54}$	125.5	95%	3%	2%	–
$H \to b\bar{b}$ (4.7 fb^{-1} at 7 TeV + 13.0 fb^{-1} at 8 TeV) [?, ?]						
VH tag	-0.39 ± 1.02	125.5	–	–	100%	–
$H \to \tau\tau$ (4.6 fb^{-1} at 7 TeV + 13.0 fb^{-1} at 8 TeV) [?]						
$\mu(\mathrm{ggF}, \tau\tau)$	2.41 ± 1.57	125	100%	–	–	–
$\mu(\mathrm{VBF} + \mathrm{VH}, \tau\tau)$	-0.26 ± 1.02	125	–	60%	40%	–

Table 1: ATLAS results as employed in this analysis. The correlations included in the fits are $\rho = -0.37$ for the $\gamma\gamma$ and $\rho = -0.50$ for the $\tau\tau$ channels.

Channel	Signal strength μ	m_H (GeV)	Production mode			
			ggF	VBF	VH	ttH
$H \to \gamma\gamma$ (5.1 fb^{-1} at 7 TeV + 5.3 fb^{-1} at 8 TeV) [?, ?, ?]						
$\mu(\mathrm{ggF} + \mathrm{ttH}, \gamma\gamma)$	0.95 ± 0.65	125.8	100%	–	–	–
$\mu(\mathrm{VBF} + \mathrm{VH}, \gamma\gamma)$	3.77 ± 1.75	125.8	–	60%	40%	–
$H \to ZZ$ (5.1 fb^{-1} at 7 TeV + 12.2 fb^{-1} at 8 TeV) [?, ?]						
Inclusive	$0.81^{+0.35}_{-0.28}$	125.8	87%	7%	5%	1%
$H \to WW$ (up to 4.9 fb^{-1} at 7 TeV + 12.1 fb^{-1} at 8 TeV) [?, ?, ?]						
0/1 jet	$0.77^{+0.27}_{-0.25}$	125.8	97%	3%	–	–
VBF tag	$-0.05^{+0.74}_{-0.55}$	125.8	17%	83%	–	–
VH tag	$-0.31^{+2.22}_{-1.94}$	125.8	–	–	100%	–
$H \to b\bar{b}$ (up to 5.0 fb^{-1} at 7 TeV + 12.1 fb^{-1} at 8 TeV) [?, ?, ?]						
VH tag	$1.31^{+0.65}_{-0.60}$	125.8	–	–	100%	–
ttH tag	$-0.80^{+2.10}_{-1.84}$	125.8	–	–	–	100%
$H \to \tau\tau$ (up to 5.0 fb^{-1} at 7 TeV + 12.1 fb^{-1} at 8 TeV) [?, ?, ?]						
0/1 jet	$0.85^{+0.68}_{-0.66}$	125.8	76%	16%	7%	1%
VBF tag	$0.82^{+0.82}_{-0.75}$	125.8	19%	81%	–	–
VH tag	$0.86^{+1.92}_{-1.68}$	125.8	–	–	100%	–

Table 2: CMS results as employed in this analysis. The correlation included for the $\gamma\gamma$ channel is $\rho = -0.54$.

Channel	Signal strength μ	m_H (GeV)	Production mode			
			ggF	VBF	VH	ttH
$H \to \gamma\gamma$ [?]						
Combined	$6.14^{+3.25}_{-3.19}$	125	78%	5%	17%	–
$H \to WW$ [?]						
Combined	$0.85^{+0.88}_{-0.81}$	125	78%	5%	17%	–
$H \to b\bar{b}$ [?]						
VH tag	$1.56^{+0.72}_{-0.73}$	125	–	–	100%	–

Table 3: Tevatron results for up to $10\ \mathrm{fb}^{-1}$ at $\sqrt{s} = 1.96$ TeV, as employed in this analysis.

Note: general enhancement of $\gamma\gamma$ final states in both ggF (not CMS) and especially VBF.

Note: $R(ZZ, WW) \gtrsim 1$ for ATLAS, whereas $R(ZZ, WW) < 1$ for CMS.

- **The big questions:**
  1. If the deviations from a single SM Higgs survive what is the model?
  2. If they do survive, how far beyond the "standard" model must we go to describe them?

Higgs coupling fits

- Suppose the signal derives from just one Higgs boson — we assume 0^+.
- The structure we will test is

$$\mathcal{L} = g\Big[C_V\left(m_W W_\mu W^\mu + \frac{m_Z}{\cos\theta_W} Z_\mu Z^\mu\right) - C_U\frac{m_t}{2m_W}\bar{t}t - C_D\frac{m_b}{2m_W}\bar{b}b - C_D\frac{m_\tau}{2m_W}\bar{\tau}\tau\Big]H\,. \quad (3)$$

  In general, the C_I can take on negative as well as positive values; there is one overall sign ambiguity which we fix by taking $C_V > 0$.
- We will be fitting the data given earlier.
- In addition to the tree-level couplings given above, the H has couplings to gg and $\gamma\gamma$ that are first induced at one loop and

are completely computable in terms of C_U, C_D and C_V if only loops containing SM particles are present.

We define $\overline{C}_g$ and $\overline{C}_\gamma$ to be the ratio of these couplings so computed to the SM ($i.e.$ $C_U = C_D = C_V = 1$) values.

- However, in some of our fits we will also allow for additional loop contributions ΔC_g and ΔC_γ from new particles; in this case $C_g = \overline{C}_g + \Delta C_g$ and $C_\gamma = \overline{C}_\gamma + \Delta C_\gamma$.
- The largest set of independent parameters in our fits is thus

$$C_U,\ C_D,\ C_V,\ \Delta C_g,\ \Delta C_\gamma\,. \tag{4}$$

- **Fit I: $C_U = C_D = C_V = 1$, ΔC_g and ΔC_γ free.**

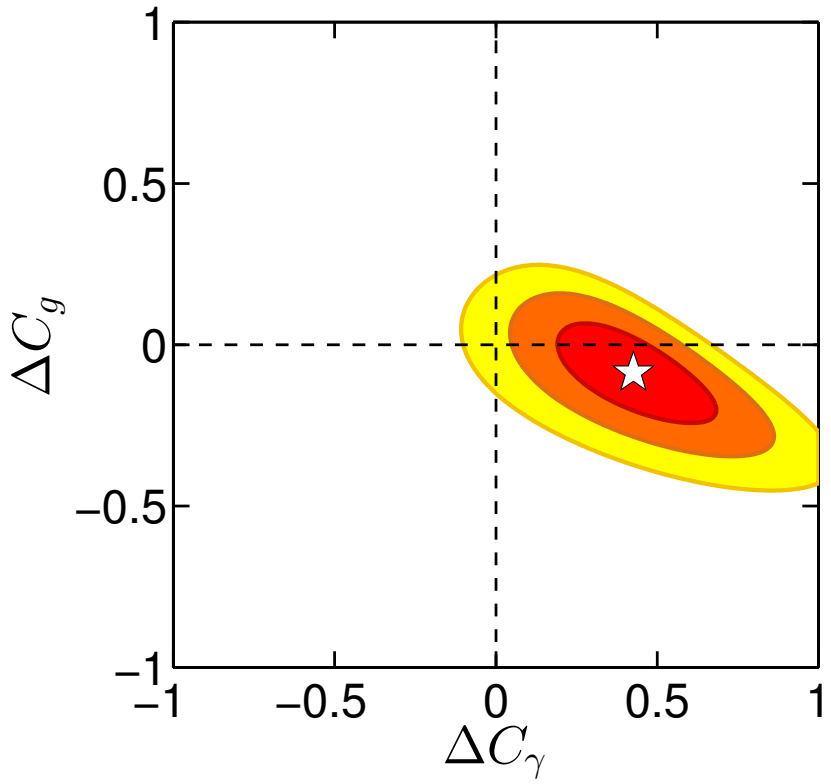

Figure 1: Two parameter fit of ΔC_γ and ΔC_g, assuming $C_U = C_D = C_V = 1$ (Fit I). The red, orange and yellow ellipses show the 68%, 95% and 99.7% CL regions, respectively. The white star marks the best-fit point $\Delta C_\gamma = 0.426$, $\Delta C_g = -0.086$. It has $\chi^2 = 12.3$ vs. SM $\chi^2 = 20.2$. i.e. SM is $\sim 2\sigma$ worse.

- **Fit II: varying C_U, C_D and C_V ($\Delta C_\gamma = \Delta C_g = 0$)**

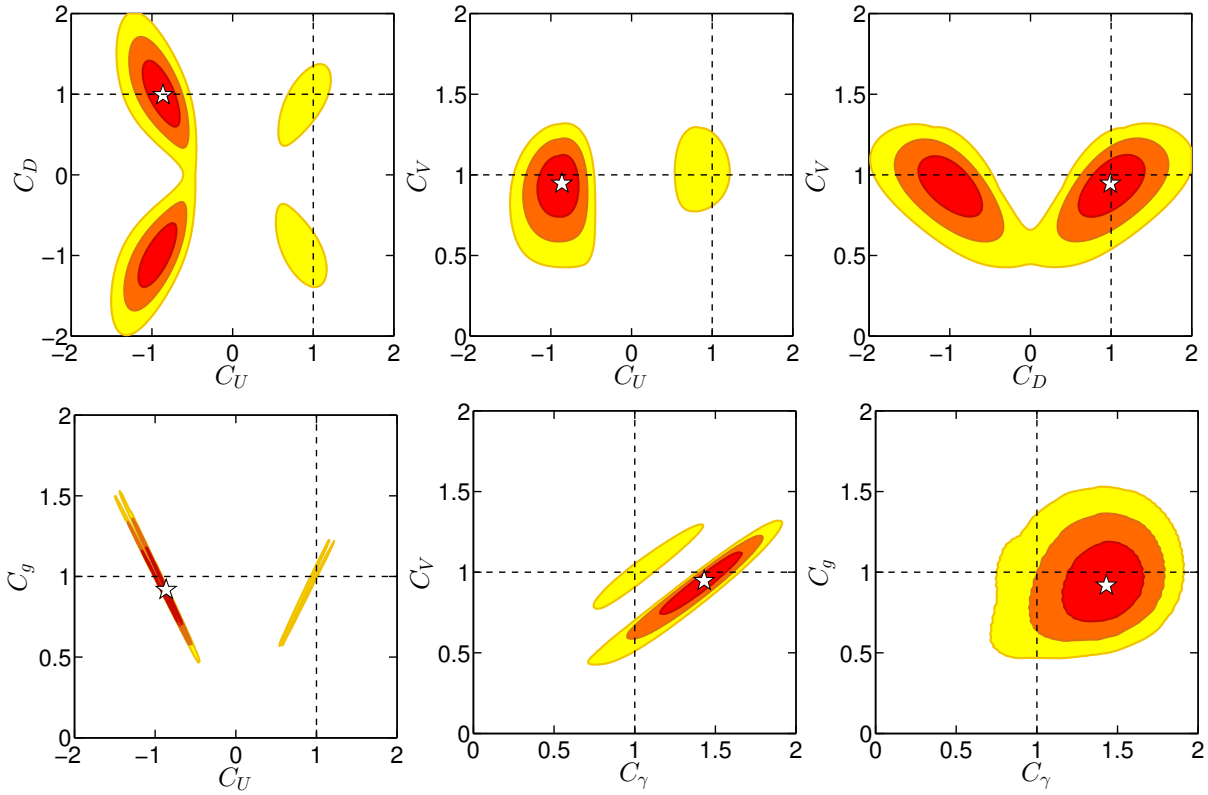

Figure 2: Two-dimensional χ^2 distributions for the three parameter fit, Fit II, of C_U, C_D, C_V with $C_\gamma = \overline{C}_\gamma$ and $C_g = \overline{C}_g$ as computed in terms of C_U, C_D, C_V. Details on the minima in different sectors of the (C_U, C_D) plane can be found in Table 5. Note strong preference for negative $C_U = -1$ ($\gamma\gamma$ t-loop adds to W loop). Negative C_U is hard in most models. But, $\chi^2 = 11.6$ is much better than for SM.

- **Fit II: varying C_U, C_D and C_V ($\Delta C_\gamma = \Delta C_g = 0$) requiring $C_U, C_D > 0$ (and $C_V > 0$ by convention)**

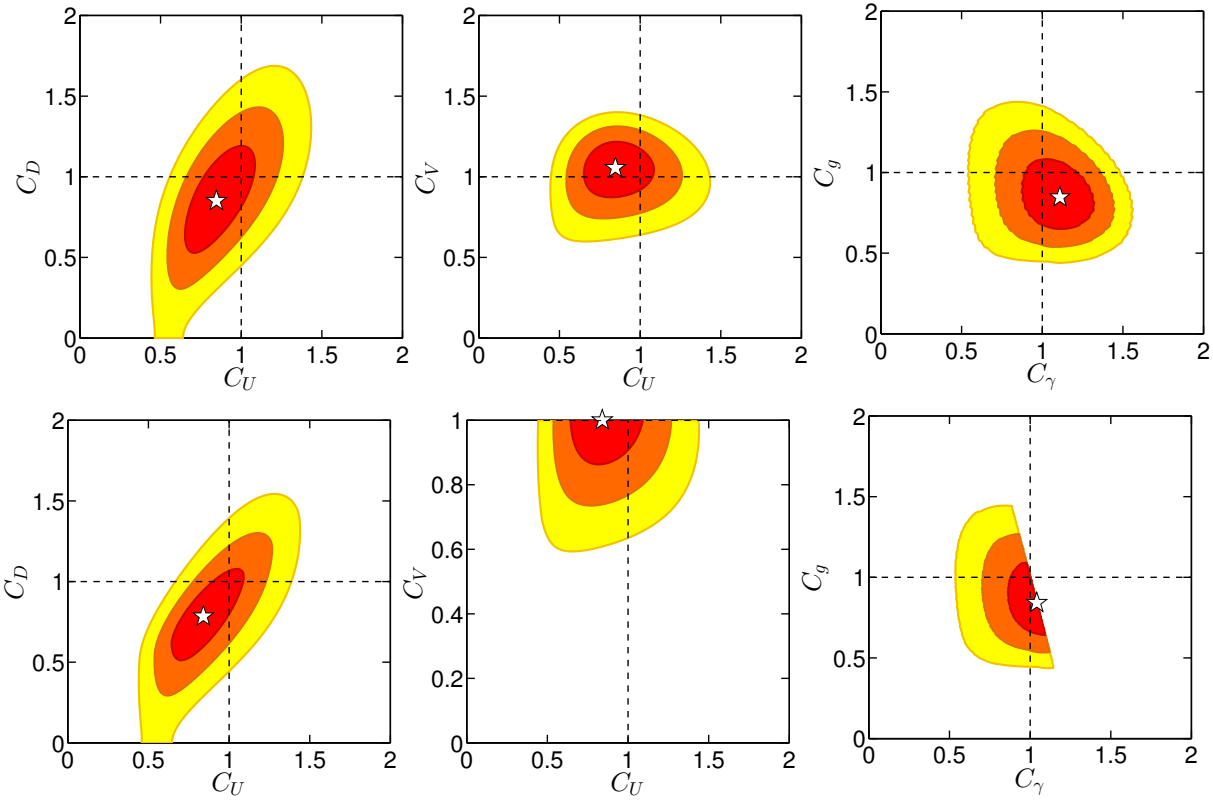

Figure 3: Two-dimensional χ^2 distributions for the three parameter fit, Fit II, as in Fig. 2 but with $C_U > 0$, $C_D > 0$, $C_V > 0$. The upper row of plots allows for $C_V > 1$, while in the lower row of plots $C_V \leq 1$ is imposed. The best fit point has $\chi^2 = 18.66$, a value that is not much lower than that for the SM.

- **Fit III: varying C_U, C_D, C_V, ΔC_γ and ΔC_g**

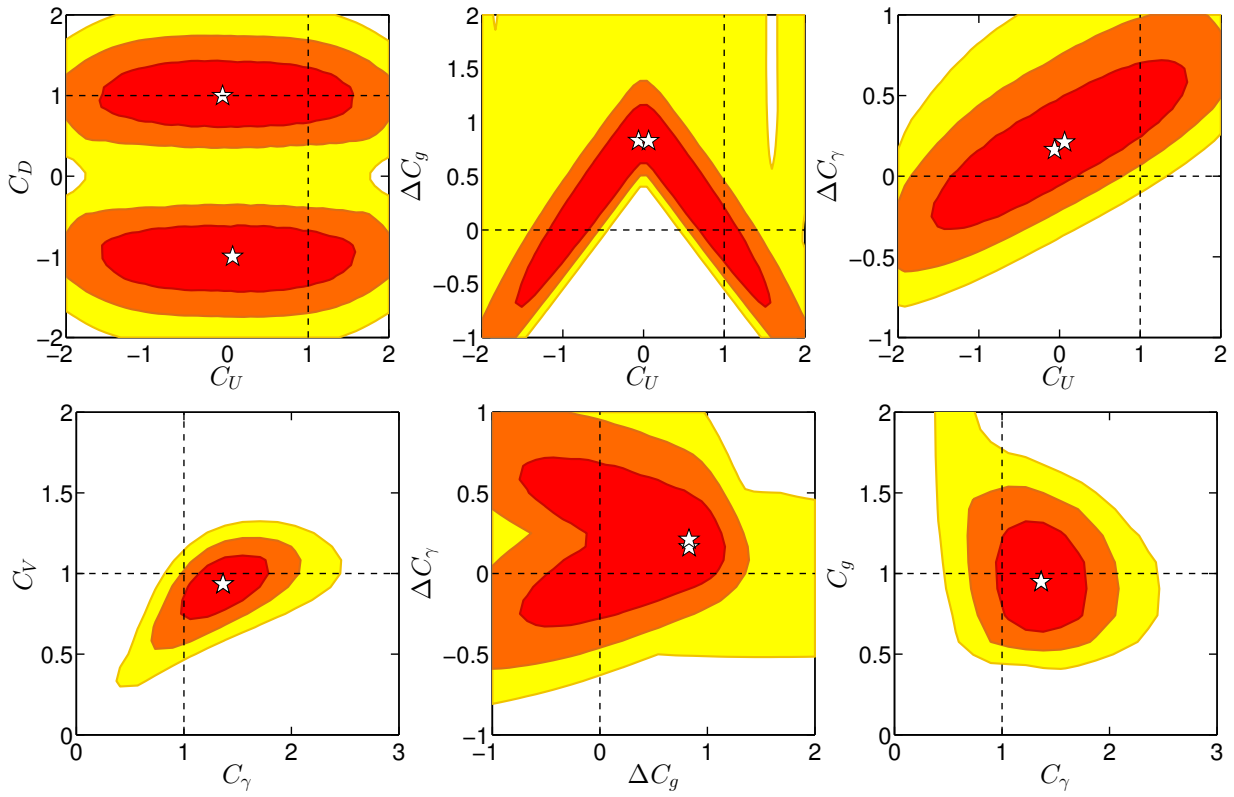

Figure 4: Two-dimensional distributions for the five parameter fit of C_U, C_D, C_V, ΔC_γ and ΔC_g (Fit III). Details regarding the best fit point are given in Table 4. Note from top middle plot how ΔC_g can be traded for C_U.

Fit	I	II	III, 1st min.	III, 2nd min.
C_U	1	$-0.864^{+0.142}_{-0.163}$	-0.06 ± 1.3	0.06 ± 1.3
C_D	1	$0.991^{+0.277}_{-0.261}$	$0.996^{+0.284}_{-0.264}$	$-0.996^{+0.263}_{-0.284}$
C_V	1	$0.947^{+0.119}_{-0.132}$	$0.934^{+0.124}_{-0.140}$	$0.934^{+0.124}_{-0.140}$
ΔC_γ	$0.426^{+0.167}_{-0.157}$	–	$0.164^{+0.380}_{-0.360}$	$0.210^{+0.372}_{-0.389}$
ΔC_g	$-0.086^{+0.102}_{-0.103}$	–	$0.830^{+0.24}_{-1.17}$	$0.828^{+0.24}_{-1.17}$
C_γ	$1.426^{+0.167}_{-0.157}$	$1.431^{+0.165}_{-0.173}$	$1.364^{+0.263}_{-0.225}$	$1.364^{+0.263}_{-0.225}$
C_g	$0.914^{+0.102}_{-0.103}$	$0.918^{+0.173}_{-0.153}$	$0.948^{+0.26}_{-0.23}$	$0.948^{+0.26}_{-0.23}$
$\chi^2_{\rm min}$	12.31	11.95	11.46	11.46
$\chi^2_{\rm min}/{\rm d.o.f.}$	0.648	0.664	0.716	0.716

Table 4: **Summary of results for Fits I–III. For Fit II, the tabulated results are from the best fit, cf. column 1 of Table 5.**

Sector	$C_U < 0, C_D > 0$	$C_U, C_D < 0$	$C_U, C_D > 0$
C_U	$-0.864^{+0.142}_{-0.163}$	$-0.911^{+0.150}_{-0.171}$	$0.847^{+0.152}_{-0.133}$
C_D	$0.991^{+0.277}_{-0.261}$	$-0.980^{+0.258}_{-0.273}$	$0.851^{+0.221}_{-0.213}$
C_V	$0.947^{+0.120}_{-0.132}$	$0.943^{+0.119}_{-0.133}$	$1.055^{+0.109}_{-0.118}$
C_γ	$1.431^{+0.165}_{-0.173}$	$1.425^{+0.163}_{-0.173}$	$1.110^{+0.145}_{-0.159}$
C_g	$0.918^{+0.173}_{-0.153}$	$0.909^{+0.168}_{-0.150}$	$0.847^{+0.159}_{-0.128}$
$\chi^2_{\rm min}$	11.95	12.06	18.66
$\chi^2_{\rm min}/{\rm d.o.f.}$	0.66	0.67	1.04

Table 5: Results for Fit II in different sectors of the (C_U, C_D) plane.

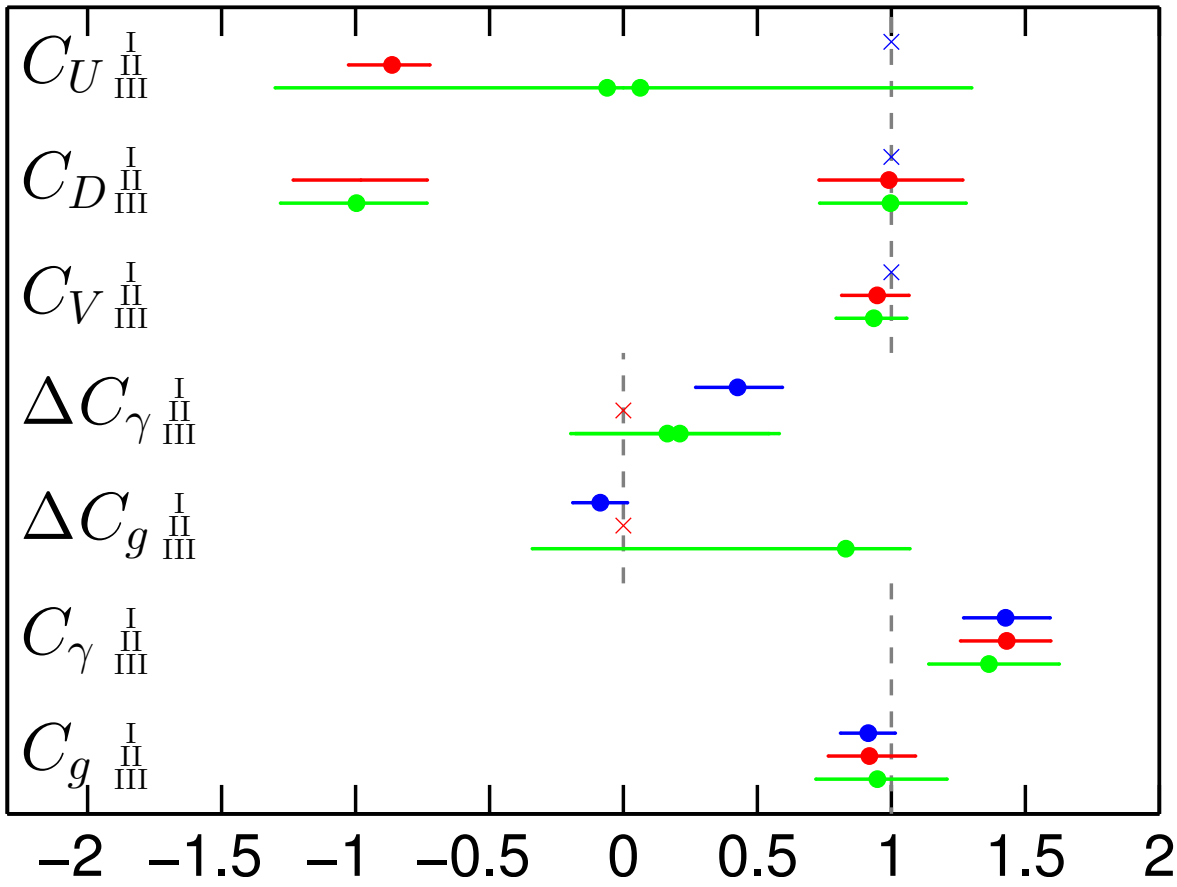

Figure 5: Graphical representation of the best fit values for C_U, C_D, C_V, ΔC_γ and ΔC_g of Table 4. The labels refer to the fits discussed in the text. The dashed lines indicate the SM value for the given quantity. The $\times$'s indicate cases where the parameter in question was fixed to its SM value. If the $\gamma\gamma$ mode excesses persist, it would appear necessary to have $C_\gamma \sim 1.4$ by some means or other (C_U negative with ΔC_γ small, or C_U normal with $\Delta C_\gamma \sim 0.4$.) Note that $C_g \sim 1$ and $C_V \sim 1$ for all fits.

Impact on Two-Higgs-Doublet Models

- **Only α and β needed to describe a single Higgs. So good fit is not exactly guaranteed.**

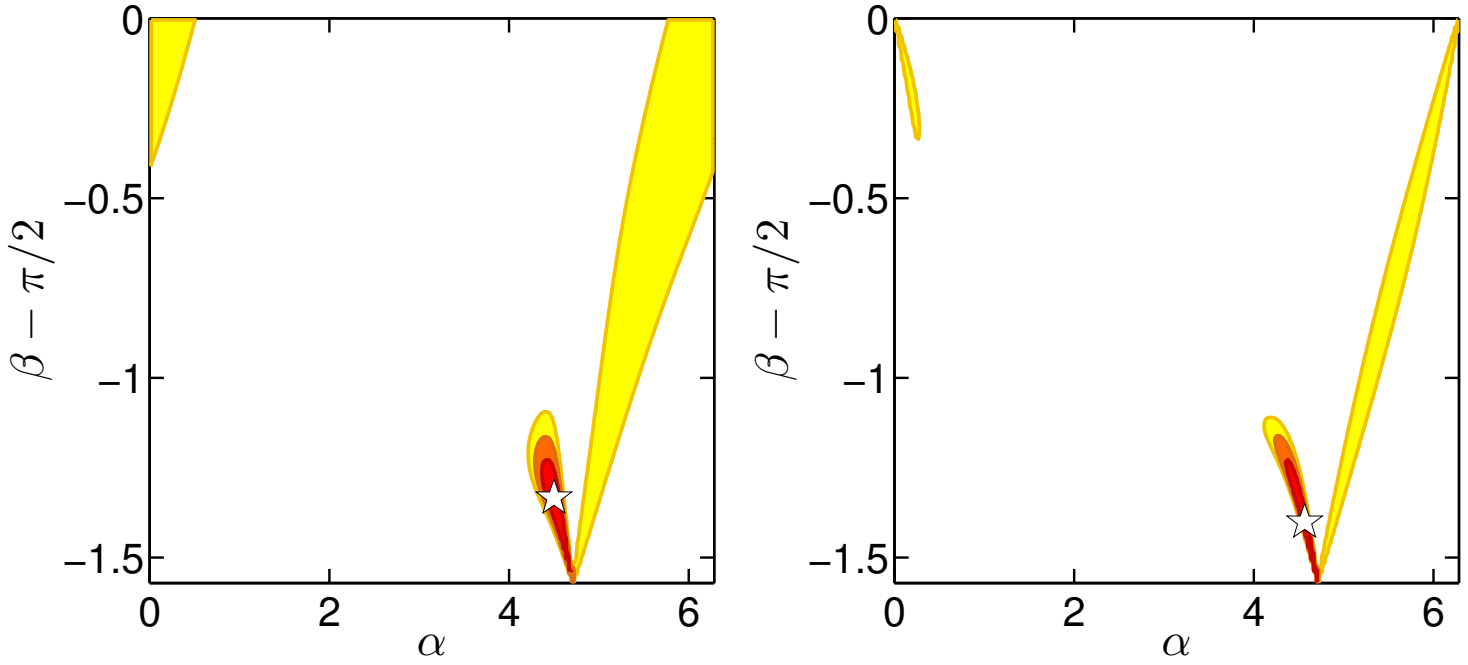

Figure 6: 2HDM fits for the h in the Type I (left) and Type II (right) models. Note: $\beta - \pi/2 = \alpha - 2\pi$ is SM limit. Fit is far from SM limit and requires small $\tan\beta$, the latter being problematical for perturbativity of top-quark coupling. If we require $\tan\beta > 1$, must move to 'long valley' which is near SM-like limit and has much higher χ^2.

Fit	THDM-I	THDM-II	THDM-I, $\tan\beta > 1$	THDM-II, $\tan\beta > 1$
α [rad]	$4.5^{+0.093}_{-0.081}$	$4.56^{+0.148}_{-0.136}$	$5.374^{+1.113}_{-0.131}$	$6.275^{+0.165}_{-0.825}$
β [rad]	$0.237^{+0.069}_{-0.097}$	$0.17^{+0.124}_{-0.170}$	$[\pi/4,\ \pi/2]$	$1.562^{+0.009}_{-0.776}$
$\cos\alpha$	$-0.211^{+0.092}_{-0.078}$	$-0.147^{+0.147}_{-0.133}$	$0.614^{+0.386}_{-0.108}$	$1.0_{-0.673}$
$\tan\beta$	$0.241^{+0.075}_{-0.101}$	$0.172^{+0.131}_{-0.172}$	$[1,\ +\infty]$	$[1,\ +\infty]$
C_U	$-0.899^{+0.166}_{-0.192}$	$-0.869^{+0.116}_{-0.134}$	$0.869^{+0.168}_{-0.154}$	$1.02^{+0.05}_{-0.07}$
C_D	$-0.899^{+0.166}_{-0.192}$	$1.004_{-0.01}$	$0.869^{+0.168}_{-0.154}$	$0.94^{+0.13}_{-0.11}$
C_V	$0.901^{+0.069}_{-0.073}$	$0.950^{+0.048}_{-0.115}$	$0.992^{+0.008}_{-0.040}$	$1.0_{-0.047}$
C_γ	$1.369^{+0.094}_{-0.097}$	$1.436^{+0.081}_{-0.130}$	$1.025_{-0.062}$	$1.005^{+0.009}_{-0.088}$
C_g	$0.899^{+0.188}_{-0.162}$	$0.924^{+0.132}_{-0.113}$	$0.869^{+0.164}_{-0.149}$	$0.99^{+0.08}_{-0.04}$
$\chi^2_{\rm min}$	12.20	11.95	19.43	19.88

Table 6: Summary of fit results for the h in 2HDMs of Type I and Type II.

Summary of Fitting Results

Best χ^2's are achieved pretty far from SM limit and would have to involve exotic parameters. One cure: light charged Higgs, but then other constraints become a problem. Second cure: degenerate Higgs bosons.

Enhanced Higgs signals in the NMSSM

- NMSSM=MSSM+$\widehat{S}$.
- The extra complex S component of $\widehat{S} \Rightarrow$ the NMSSM has h_1, h_2, h_2, a_1, a_2.
- The new NMSSM parameters of the superpotential (λ and κ) and scalar potential (A_λ and A_κ) appear as:

$$W \ni \lambda \widehat{S}\widehat{H}_u\widehat{H}_d + \frac{\kappa}{3}\widehat{S}^3\,, \quad V_{\rm soft} \ni \lambda A_\lambda S H_u H_d + \frac{\kappa}{3} A_\kappa S^3 \quad (5)$$

- $\langle S\rangle \neq 0$ is generated by SUSY breakng and solves μ problem: $\mu_{\rm eff} = \lambda\langle S\rangle$.
- First question: Can the NMSSM give a Higgs mass as large as 125 GeV?

  Answer: Yes, so long as it is not a highly unified model. For our studies, we employed universal m_0, except for NUHM ($m^2_{H_u}$,

$m^2_{H_d}$, m^2_S free), universal $A_t = A_b = A_\tau = A_0$ but allow A_λ and A_κ to vary freely. Of course, $\lambda > 0$ and κ are scanned demanding perturbativity up to the GUT scale.

- Can this model achieve rates in $\gamma\gamma$ and 4ℓ that are $>$SM?
  Answer: it depends on whether or not we insist on getting good a_μ.
- The possible mechanism (arXiv:1112.3548, Ellwanger) is to reduce the $b\bar{b}$ width of the mainly SM-like Higgs by giving it some singlet component. The gg and $\gamma\gamma$ couplings are less affected.
- Typically, this requires m_{h_1} and m_{h_2} to have similar masses (for singlet-doublet mixing) and large λ (to enhance Higgs mass). Large λ (by which we mean $\lambda > 0.1$) is only possible while retaining perturbativity up to m_{Pl} if $\tan\beta$ is modest in size. In the semi-unified model we employ, enhanced rates and/or large λ cannot be made consistent with decent δa_μ. (J. F. Gunion, Y. Jiang and S. Kraml.arXiv:1201.0982 [hep-ph])

- **The "enhanced" SM-like Higgs can be either h_1 or h_2.**

$$R_{gg}^{h_i}(X) \equiv (C_{gg}^{h_i})^2 \frac{\mathrm{BR}(h_i \to X)}{\mathrm{BR}(h_{SM} \to X)}, \quad R_{\mathrm{VBF}}^{h_i}(X) \equiv (C_{VV}^{h_i})^2 \frac{\mathrm{BR}(h_i \to X)}{\mathrm{BR}(h_{SM} \to X)}, \quad (6)$$

where h_i is the i^{th} NMSSM scalar Higgs, and h_{SM} is the SM Higgs boson. $C_Y^{h_i} = g_{Y h_i}/g_{Y h_{SM}}$ and R_{Vh} for $V^* \to V h_i$ ($V = W, Z$) with $h_i \to X$ is equal to $R_{\mathrm{VBF}}^{h_i}(X)$ *in doublets + singlets models*.

Some illustrative R_{gg} results from (J. F. Gunion, Y. Jiang and S. Kraml. arXiv:1207.1545):

Figure Legend

	LEP/Teva	B-physics	$\Omega h^2 > 0$	$\delta a_\mu (\times 10^{10})$	XENON100	$R^{h_1/h_2}(\gamma\gamma)$
●	$\surd$	$\surd$	$0 - 0.136$	$\times$	$\surd$	$[0.5, 1]$
■	$\surd$	$\surd$	$0 - 0.094$	$\times$	$\surd$	$(1, 1.2]$
▲	$\surd$	$\surd$	$0 - 0.094$	$\times$	$\surd$	> 1.2
■	$\surd$	$\surd$	0.094-0.136	$\times$	$\surd$	$(1, 1.2]$
▲	$\surd$	$\surd$	0.094-0.136	$\times$	$\surd$	> 1.2
♦	$\surd$	$\surd$	$0.094 - 0.136$	4.27-49.1	$\surd$	~ 1

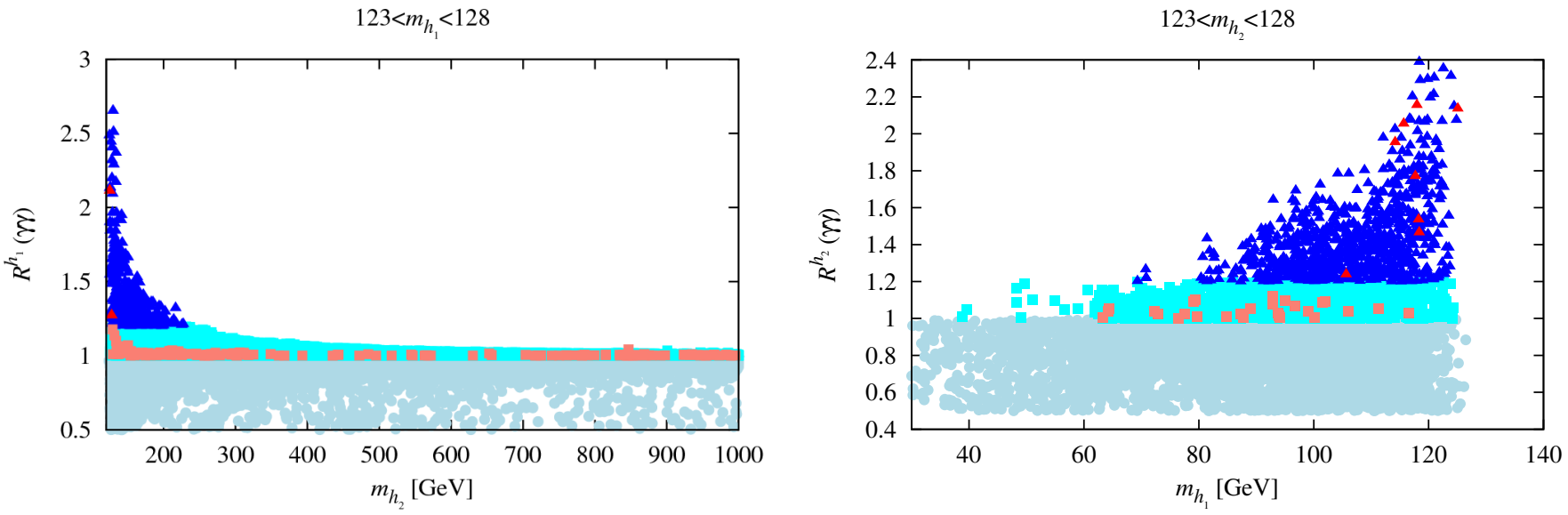

Figure 7: The plot shows $R_{gg}(\gamma\gamma)$ for the cases of $123 < m_{h_1} < 128$ GeV and $123 < m_{h_2} < 128$ GeV. Note: red triangle (orange square) is for WMAP window with $R_{gg}(\gamma\gamma) > 1.2$ ($R_{gg}(\gamma\gamma) = [1, 1.2]$).

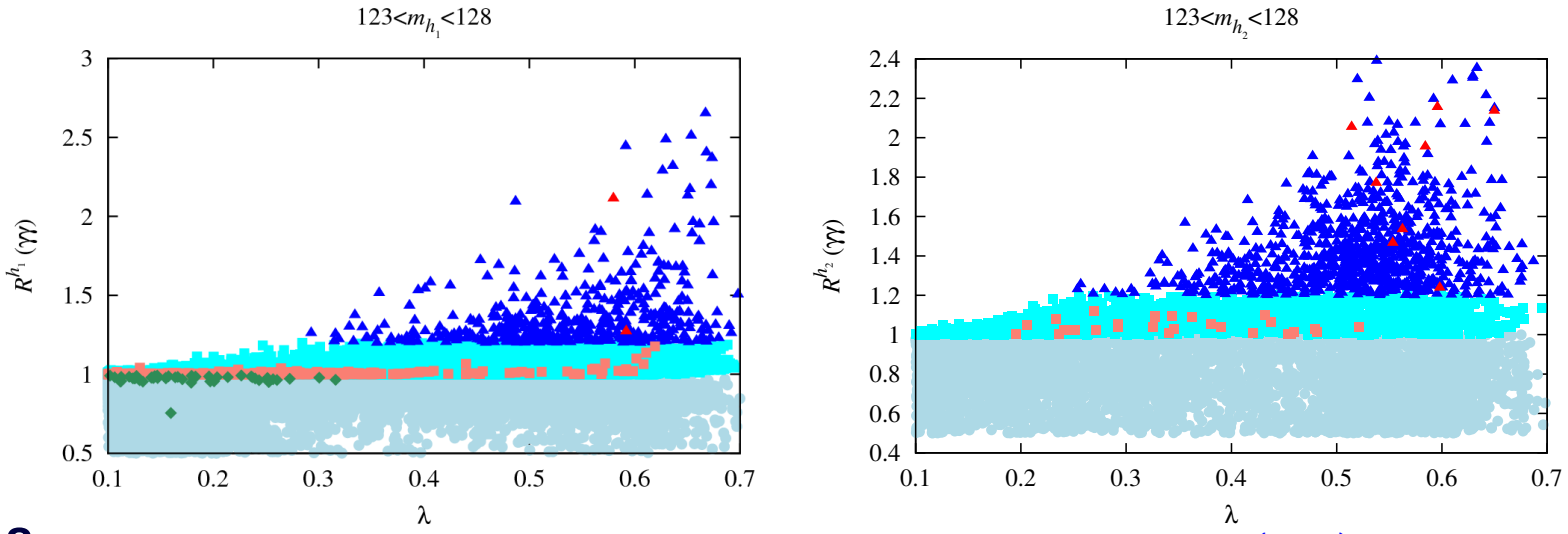

Figure 8: Observe the clear general increase in maximum $R_{gg}(\gamma\gamma)$ with increasing λ. Green points have good δa_μ, $m_{h_2} > 1$ TeV BUT $R_{gg}(\gamma\gamma) \sim 1$.

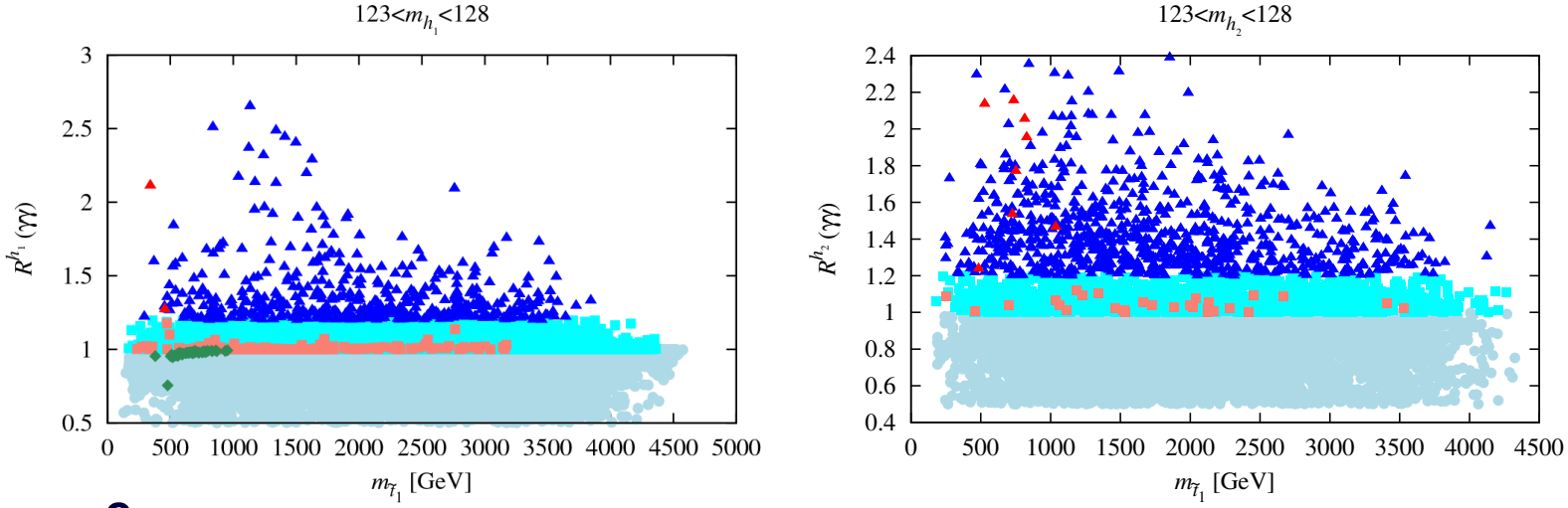

Figure 9: The lightest stop has mass $\sim 300 - 700$ GeV for red-triangle points.

- **If we ignore δa_μ, then $R_{gg}(\gamma\gamma) > 1.2$ (even > 2) is possible while satisfying all other constraints provided h_1 and h_2 are close in mass, especially in the case where $m_{h_2} \in [123, 128]$ GeV window.**
- **This raises the issue of scenarios in which *both* m_{h_1} and m_{h_2} are in the $[123, 128]$ GeV window where the experiments see the Higgs signal.**

  Supporting reasons:

  - **If h_1 and h_2 are sufficiently degenerate, the experimentalists might not have resolved the two distinct peaks, even in the $\gamma\gamma$ channel.**
  - **The rates for the h_1 and h_2 could then add together to give an enhanced $\gamma\gamma$, for example, signal.**
  - **The apparent width or shape of the $\gamma\gamma$ mass distribution could be altered.**
  - **There is more room for an apparent mismatch between the**

$\gamma\gamma$ channel and other channels, such as $b\bar{b}$ or 4ℓ, than in non-degenerate situation.

In particular, the h_1 and h_2 will generally have different gg and VV production rates and branching ratios.

– The general coupling analysis suggests that suppressing the VV coupling and the $b\bar{b}$ coupling through mixing does not provide a wonderful fit if only one of the h_1 or h_2 is identified as the 126 GeV resonance.

Degenerate NMSSM Higgs Scenarios:

(arXiv:1207.1545, JFG, Jiang, Kraml)

- For the numerical analysis, we use NMSSMTools version 3.2.0, which has improved convergence of RGEs in the case of large Yukawa couplings.
- The precise constraints imposed are the following.
  1. Basic constraints: proper RGE solution, no Landau pole, neutralino LSP, Higgs and SUSY mass limits as implemented in NMSSMTools-3.2.0.
  2. B physics: $\mathrm{BR}(B_s \to X_s\gamma)$, ΔM_s, ΔM_d, $\mathrm{BR}(B_s \to \mu^+\mu^-)$ (old upper limit), $\mathrm{BR}(B^+ \to \tau^+\nu_\tau)$ and $\mathrm{BR}(B \to X_s\mu^+\mu^-)$ at 2σ as encoded in NMSSMTools-3.2.0, plus updates.
  3. Dark Matter: $\Omega h^2 < 0.136$, thus allowing for scenarios in which the relic density arises at least in part from some other source.

However, we single out points with $0.094 \leq \Omega h^2 \leq 0.136$, which is the 'WMAP window' defined in NMSSMTools-3.2.0.

4. 2011 XENON 100: spin-independent LSP–proton scattering cross section bounds implied by the neutralino-mass-dependent XENON100 bound. (For points with $\Omega h^2 < 0.094$, we rescale these bounds by a factor of $0.11/\Omega h^2$.) (2012 XENON 100 has little additional impact.)
5. δa_μ ignored: impossible to satisfy for scenarios we study here.

- Compute the effective Higgs mass in given production and final decay channels Y and X, respectively, and R^h_{gg} as

$$m_h^Y(X) \equiv \frac{R_Y^{h_1}(X) m_{h_1} + R_Y^{h_2}(X) m_{h_2}}{R_Y^{h_1}(X) + R_Y^{h_2}(X)} \qquad R_Y^h(X) = R_Y^{h_1}(X) + R_Y^{h_2}(X)\,. \tag{7}$$

- The extent to which it is appropriate to combine the rates from the h_1 and h_2 depends upon the degree of degeneracy and the

experimental resolution.

Very roughly, one should probably think of $\sigma_{\rm res} \sim 1.5$ GeV or larger. The widths of the h_1 and h_2 are very much smaller than this resolution.

- We perform scans covering the following parameter ranges:

$$0 \leq m_0 \leq 3000; \quad 100 \leq m_{1/2} \leq 3000; \quad 1 \leq \tan\beta \leq 40;$$
$$-6000 \leq A_0 \leq 6000; 0.1 \leq \lambda \leq 0.7; \quad 0.05 \leq \kappa \leq 0.5;$$
$$-1000 \leq A_\lambda \leq 1000; \quad -1000 \leq A_\kappa \leq 1000; \quad 100 \leq \mu_{eff} \leq 500\,. \qquad (8)$$

We only display points which pass the basic constraints, satisfy B-physics constraints, have $\Omega h^2 < 0.136$, obey the 2011 XENON100 limit on the LSP scattering cross-section off protons *and* have *both* h_1 and h_2 in the desired mass range: 123 GeV $< m_{h_1}, m_{h_2} < 128$ GeV.

- In Fig. 10, points are color coded according to $m_{h_2} - m_{h_1}$. Circular points have $\Omega h^2 < 0.094$, while diamond points have $0.094 \leq \Omega h^2 \leq 0.136$ (*i.e.* lie within the WMAP window).

- **Many of the displayed points have $R_{gg}^{h_1}(\gamma\gamma) + R_{gg}^{h_2}(\gamma\gamma) > 1$.**

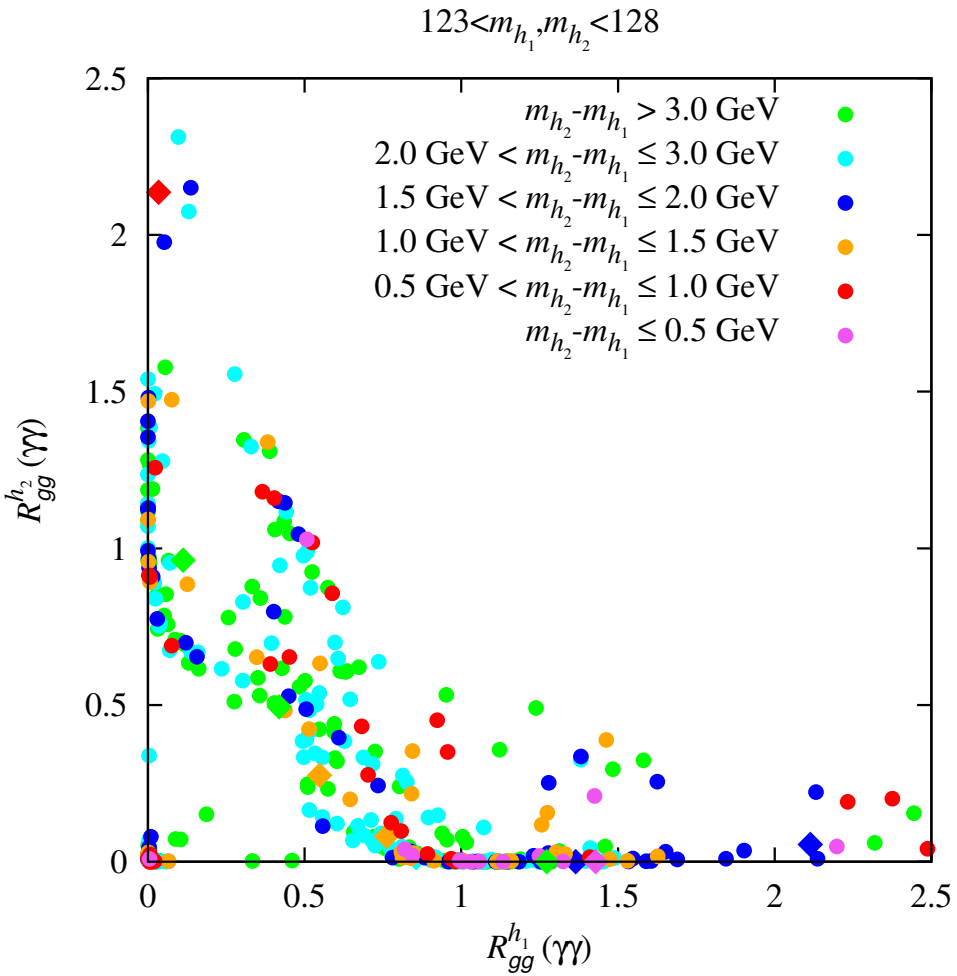

Figure 10: Correlation of $gg \to (h_1, h_2) \to \gamma\gamma$ signal strengths when both h_1 and h_2 lie in the 123–128 GeV mass range. The circular points have $\Omega h^2 < 0.094$, while diamond points have $0.094 \leq \Omega h^2 \leq 0.136$. Points are color coded according to $m_{h_2} - m_{h_1}$. Probably green and cyan points can be resolved in mass.

- A few such points have Ωh^2 in the WMAP window. These points are such that either $R_{gg}^{h_1}(\gamma\gamma) > 2$ or $R_{gg}^{h_2}(\gamma\gamma) > 2$, with the $R_{gg}^{h_2}(\gamma\gamma)$ or $R_{gg}^{h_1}(\gamma\gamma)$, respectively, being small.
- However, the majority of the points with $R_{gg}^{h_1}(\gamma\gamma)+R_{gg}^{h_2}(\gamma\gamma) > 1$ have $\Omega h^2 < 0.094$ and the $\gamma\gamma$ signal is often shared between the h_1 and the h_2.

Now combine the h_1 and h_2 signals as described above. Recall: circular (diamond) points have $\Omega h^2 < 0.094$ ($0.094 \leq \Omega h^2 \leq 0.136$). Color code:

1. red for $m_{h_2} - m_{h_1} \leq 1$ GeV;
2. blue for 1 GeV $< m_{h_2} - m_{h_1} \leq 2$ GeV;
3. green for 2 GeV $< m_{h_2} - m_{h_1} \leq 3$ GeV.

- For current statistics and $\sigma_{\rm res} \gtrsim 1.5$ GeV we estimate that the h_1 and h_2 signals will not be seen separately for $m_{h_2} - m_{h_1} \leq 2$ GeV.

- In Fig. 11, we show results for $R^h_{gg}(X)$ for $X = \gamma\gamma, VV, b\bar{b}$. Enhanced $\gamma\gamma$ and VV rates from gluon fusion are very common.
- The bottom-right plot shows that enhancement in Vh with $h \to b\bar{b}$ rate is also natural, though not as large as the best fit value suggested by the new Tevatron analysis.
- Diamond points ($i.e.$ those in the WMAP window) are rare, but typically show enhanced rates.

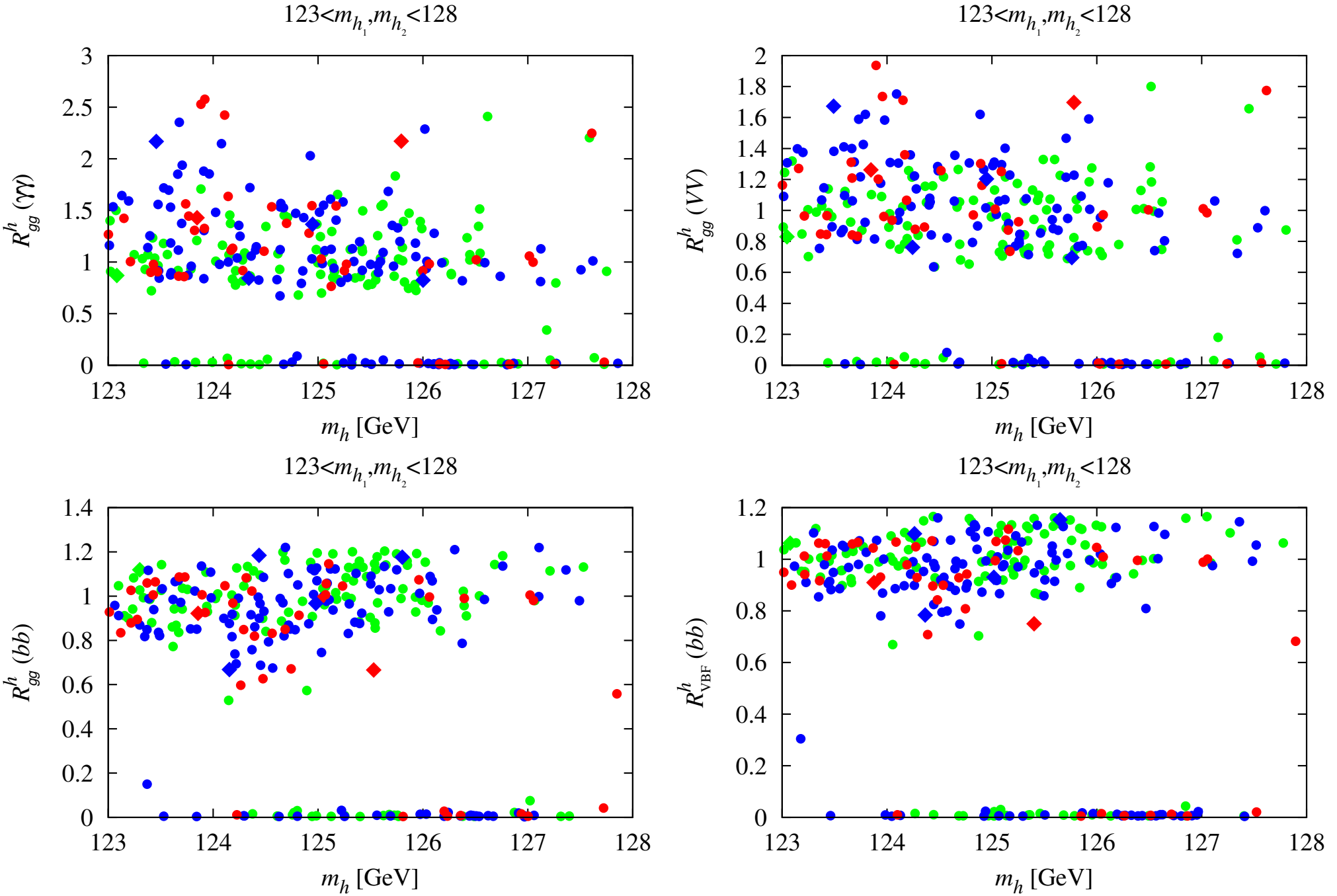

Figure 11: $R^h_{gg}(X)$ **for** $X = \gamma\gamma, VV, b\bar{b}$**, and** $R^h_{\rm VBF}(b\bar{b})$ **versus** m_h**. For application to the Tevatron, note that** $R^h_{\rm VBF}(b\bar{b}) = R^h_{V^*\to Vh}(b\bar{b})$**.**

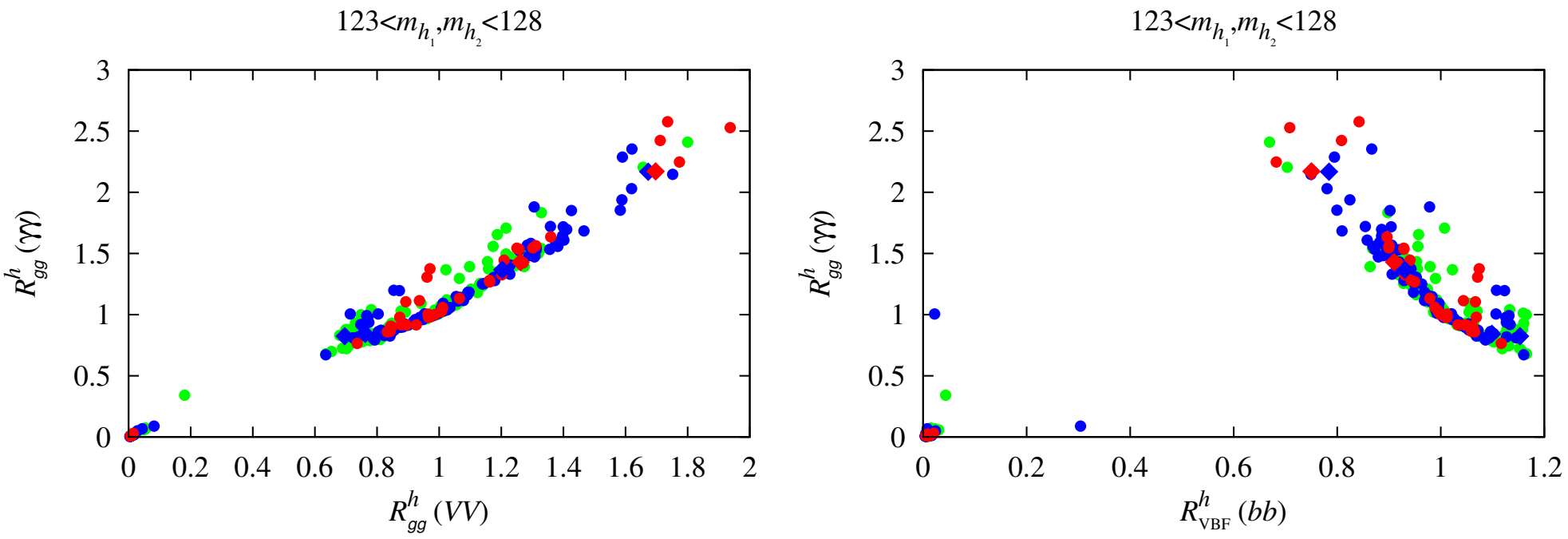

Figure 12: Left: correlation between the gluon fusion induced $\gamma\gamma$ and VV rates relative to the SM. Right: correlation between the gluon fusion induced $\gamma\gamma$ rate and the VV fusion induced $b\bar{b}$ rates relative to the SM; the relative rate for $V^* \to Vh$ with $h \to b\bar{b}$ (relevant for the Tevatron) is equal to the latter.

- **Comments on Fig. 12:**
  1. Left-hand plot shows the strong correlation between $R^h_{gg}(\gamma\gamma)$ and $R^h_{gg}(VV)$.

Note that if $R^h_{gg}(\gamma\gamma) \sim 1.5$, as suggested by current experimental results, then in this model $R^h_{gg}(VV) \geq 1.2$.

2. The right-hand plot shows the (anti) correlation between $R^h_{gg}(\gamma\gamma)$ and $R^h_{V^*\to Vh}(b\bar{b}) = R^h_{\rm VBF}(b\bar{b})$.
   In general, the larger $R^h_{gg}(\gamma\gamma)$ is, the smaller the value of $R^h_{V^*\to Vh}(b\bar{b})$.
   However, this latter plot shows that there *are* parameter choices for which both the $\gamma\gamma$ rate at the LHC and the $V^* \to Vh(\to b\bar{b})$ rate at the Tevatron (and LHC) can be enhanced relative to the SM as a result of there being contributions to these rates from both the h_1 and h_2.
3. It is often the case that one of the h_1 or h_2 dominates $R^h_{gg}(\gamma\gamma)$ while the other dominates $R^h_{V^*\to Vh}(b\bar{b})$. This is typical of the diamond WMAP-window points.
   However, a significant number of the circular $\Omega h^2 < 0.094$ points are such that either the $\gamma\gamma$ or the $b\bar{b}$ signal receives

substantial contributions from both the h_1 and the h_2. We did not find points where the $\gamma\gamma$ and $b\bar{b}$ final states *both* receive substantial contributions from *both* the h_1 and h_2.

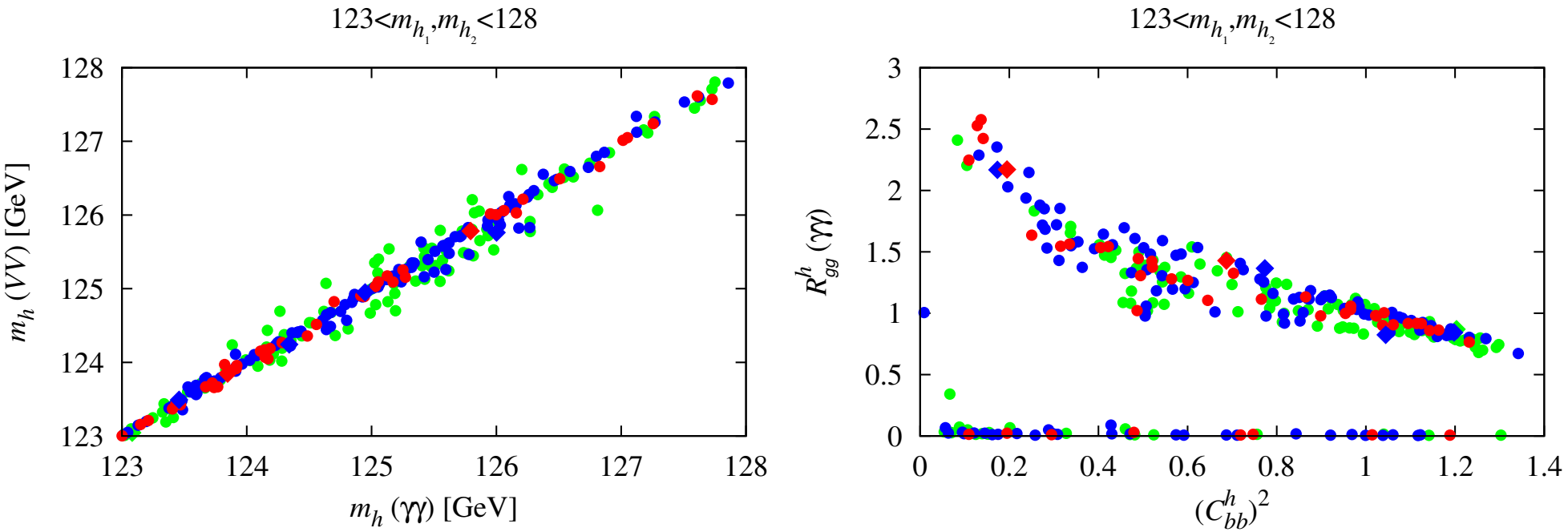

Figure 13: **Left: effective Higgs masses obtained from different channels: $m_h^{gg}(\gamma\gamma)$ versus $m_h^{gg}(VV)$. Right: $\gamma\gamma$ signal strength $R^h_{gg}(\gamma\gamma)$ versus effective coupling to $b\bar{b}$ quarks $(C^h_{b\bar{b}})^2$. Here, $C^h_{b\bar{b}}{}^2 \equiv \left[R^{h_1}_{gg}(\gamma\gamma)C^{h_1}_{b\bar{b}}{}^2 + R^{h_2}_{gg}(\gamma\gamma)C^{h_2}_{b\bar{b}}{}^2\right] / \left[R^{h_1}_{gg}(\gamma\gamma) + R^{h_2}_{gg}(\gamma\gamma)\right]$.**

Comments on Fig. 13

1. The m_h values for the gluon fusion induced $\gamma\gamma$ and VV cases are also strongly correlated — in fact, they differ by no more than a fraction of a GeV and are most often much closer, see the left plot of Fig. 13.
2. The right plot of Fig. 13 illustrates the mechanism behind enhanced rates, namely that large net $\gamma\gamma$ branching ratio is achieved by reducing the average total width by reducing the average $b\bar{b}$ coupling strength.

Separate Mass Peaks for ZZ vs. $\gamma\gamma$

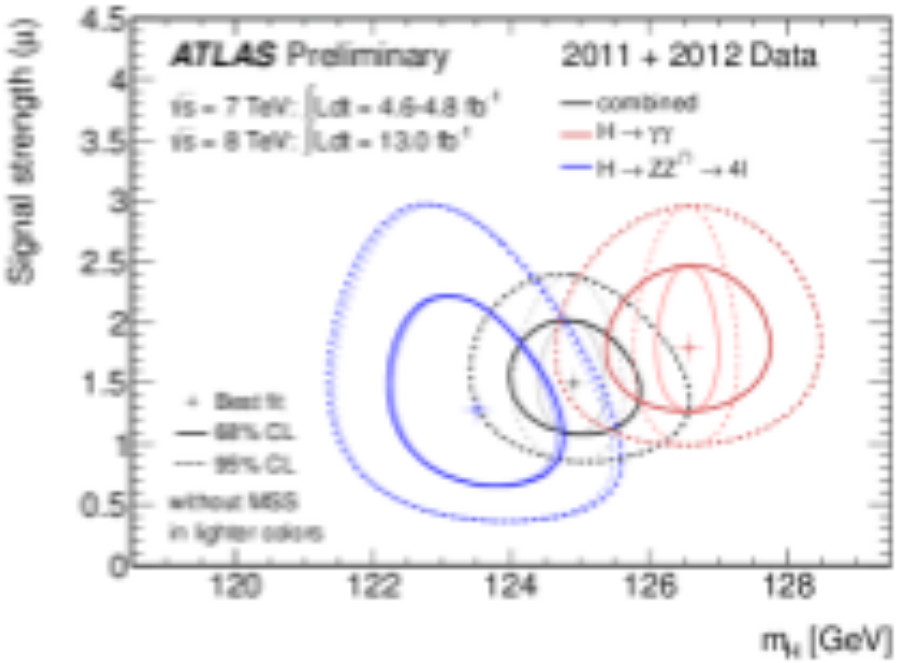

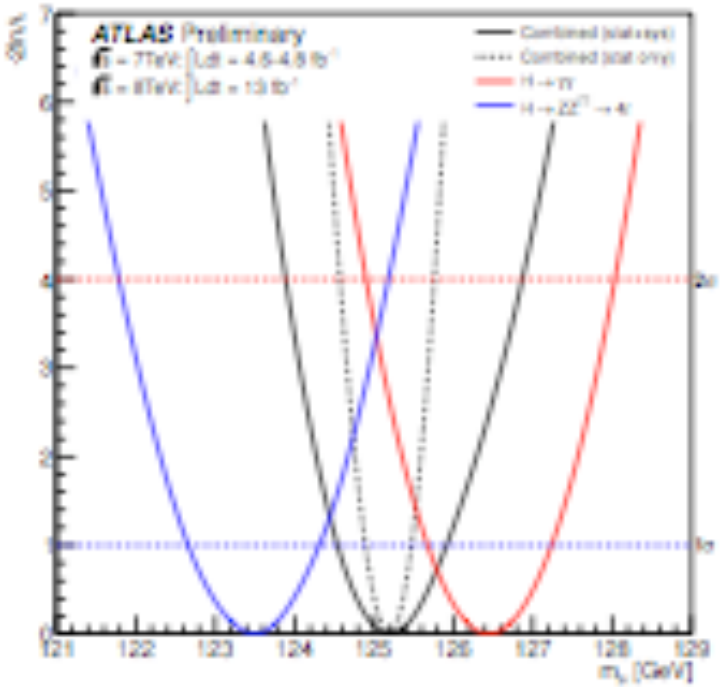

- h_1 should have $m_{h_1} \sim 123$ GeV and ZZ rate not too much smaller than SM-like rate, but suppressed $\gamma\gamma$ rate.
- h_2 should have $m_{h_2} \sim 126$ GeV and enhanced $\gamma\gamma$ and somewhat suppressed ZZ rate.

- **The kind of extreme apparently seen by ATLAS is hard to arrange in the NMSSM.**

  This is because the mechanism for getting enhanced $\gamma\gamma$ (suppression of bb partial width through mixing) automatically also enhances ZZ. Recall the correlation plot given earlier

- **To assess a bit more quantitatively, we compute $m_h(VV)$ vs. $m_h(\gamma\gamma)$ using previous formula involving weighting by $R_{gg}^{h_1,h_2}(ZZ)$ and $R_{gg}^{h_1,h_2}(\gamma\gamma)$ and accepting points with 121 GeV $\leq m_{h_1},, m_{h_2} \leq 128$ GeV.**

  Or, selecting points with 122 GeV $< m_{h_1} < 124$ GeV and 125 GeV $< m_{h_2} < 127$ GeV.

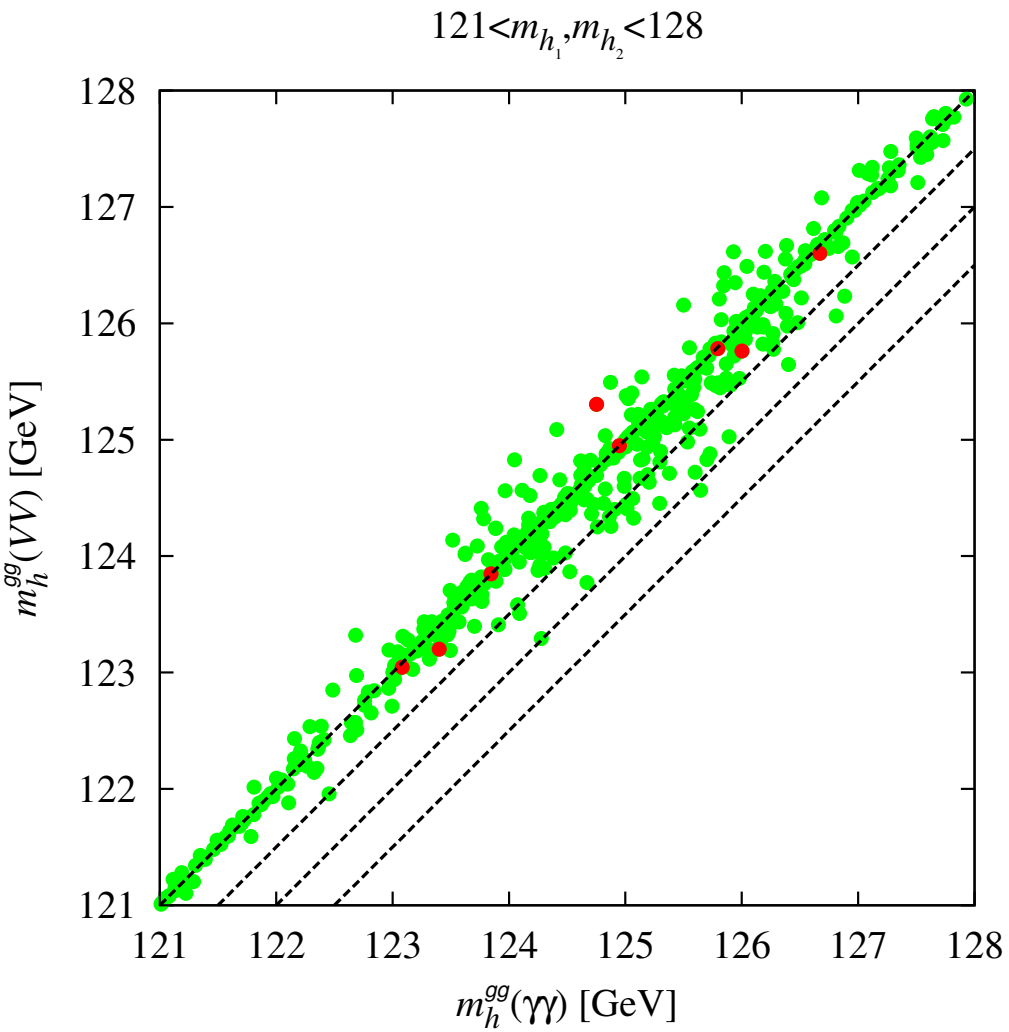

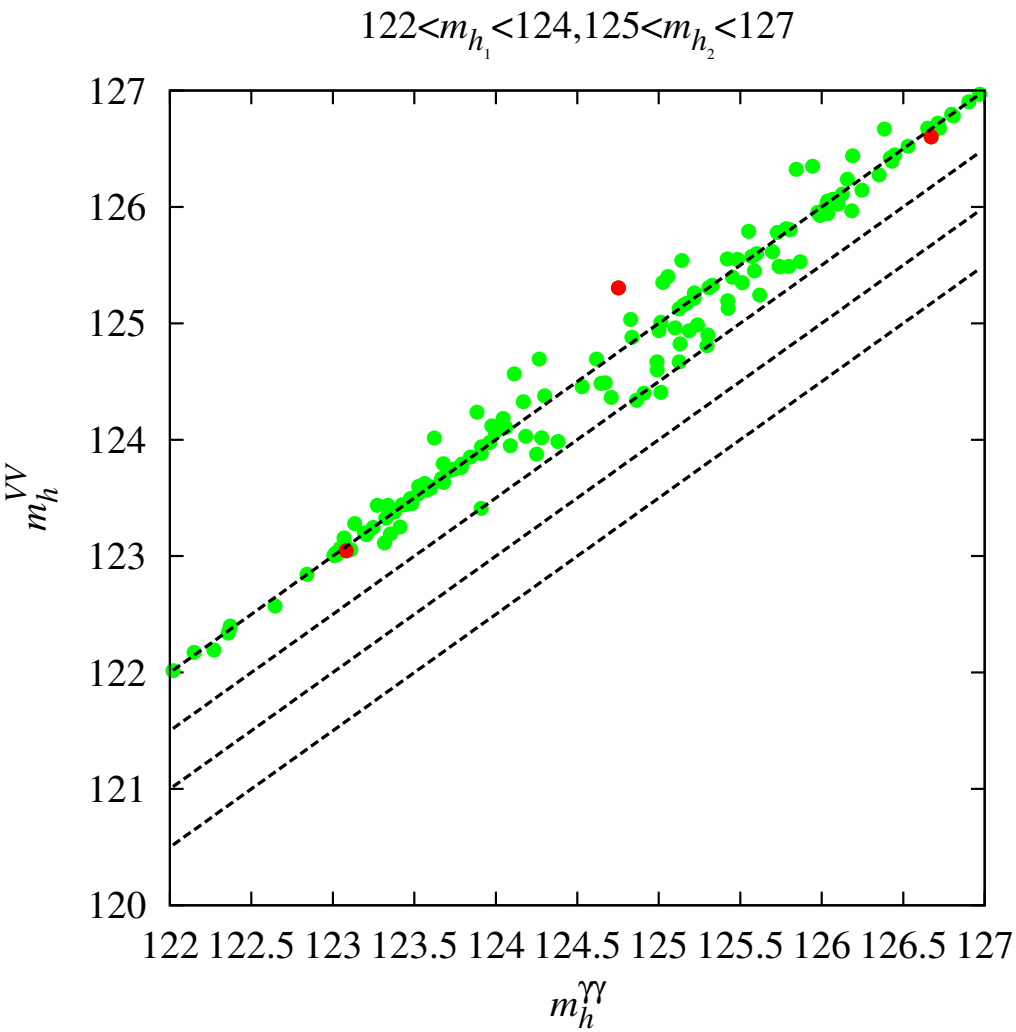

Figure 14: m_h **obtained in** ZZ **vs.** $\gamma\gamma$ **final state when scanning and requiring:** $121\ \text{GeV} \leq m_{h_1}, m_{h_2} \leq 128\ \text{GeV}$ **(Left) or** $122\ \text{GeV} < m_{h_1} < 124\ \text{GeV}$, $125\ \text{GeV} < m_{h_2} < 127\ \text{GeV}$ **(Right). Dashed lines show** $m_h(ZZ) = m_h(\gamma\gamma) - (0, 0.5, 1, 1.5)$. **Hard to get a mass shift of more than** $1\ \text{GeV}$.

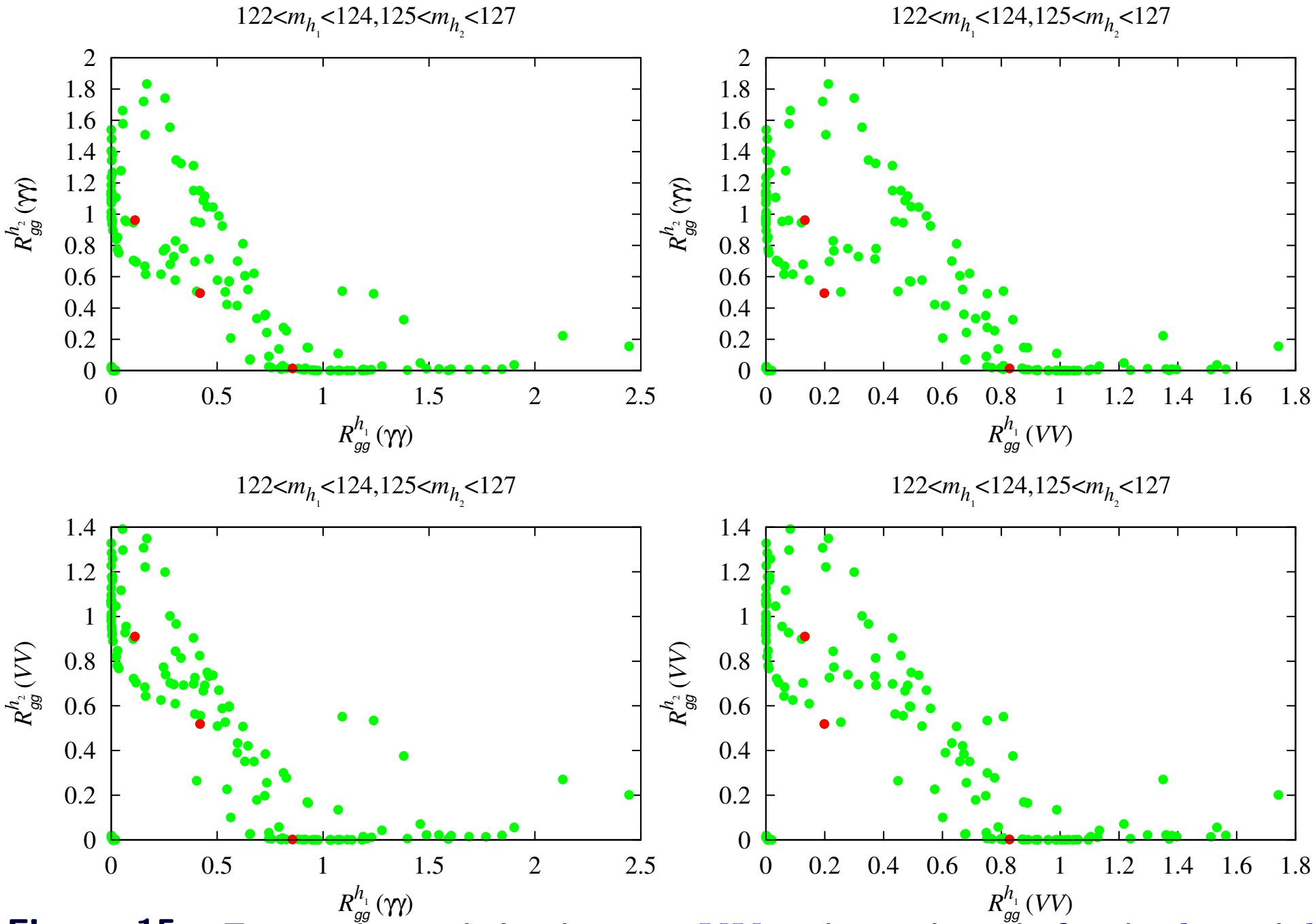

Figure 15: Too much correlation between VV and $\gamma\gamma$ channels for the h_1 and h_2 separately.

Diagnosing the presence of degenerate Higgses

(J. F. Gunion, Y. Jiang and S. Kraml. arXiv:1208.1817)

- Given that enhanced R^h_{gg} is very natural if there are degenerate Higgs mass eigenstates, how do we detect degeneracy if closely degenerate? Must look at correlations among different R^h's.
- In the context of any doublets plus singlets model not all the R^{h_i}'s are independent; a complete independent set of R^h's can be taken to be:

$$R^h_{gg}(VV),\quad R^h_{gg}(bb),\quad R^h_{gg}(\gamma\gamma),\quad R^h_{VBF}(VV),\quad R^h_{VBF}(bb),\quad R^h_{VBF}(\gamma\gamma)\,. \tag{9}$$

- Let us now look in more detail at a given $R^h_Y(X)$. It takes the form

$$R^h_Y(X) = \sum_{i=1,2} \frac{(C^{h_i}_Y)^2 (C^{h_i}_X)^2}{C^{h_i}_\Gamma} \tag{10}$$

where $C^{h_i}_X$ for $X = \gamma\gamma, WW, ZZ, \ldots$ is the ratio of the $h_i X$

to $h_{SM}X$ coupling and $C_\Gamma^{h_i}$ is the ratio of the total width of the h_i to the SM Higgs total width.

- The diagnostic tools that can reveal the existence of a second, quasi-degenerate (but non-interfering in the small width approximation) Higgs state are the double ratios:

$$\text{I):}\ \frac{R^h_{VBF}(\gamma\gamma)/R^h_{gg}(\gamma\gamma)}{R^h_{VBF}(bb)/R^h_{gg}(bb)},\quad \text{II):}\ \frac{R^h_{VBF}(\gamma\gamma)/R^h_{gg}(\gamma\gamma)}{R^h_{VBF}(VV)/R^h_{gg}(VV)},\quad \text{III):}\ \frac{R^h_{VBF}(VV)/R^h_{gg}(VV)}{R^h_{VBF}(bb)/R^h_{gg}(bb)}, \tag{11}$$

each of which should be unity if only a single Higgs boson is present but, due to the non-factorizing nature of the sum in Eq. (10), are generally expected to deviate from 1 if two (or more) Higgs bosons are contributing to the net h signals.

- In a doublets+singlets model all other double ratios that are equal to unity for single Higgs exchange are not independent of the above three.
- Of course, the above three double ratios are not all independent. Which will be most useful depends upon the precision with

which the R^h's for different initial/final states can be measured. E.g measurements of R^h for the bb final state may continue to be somewhat imprecise and it is then double ratio II) that might prove most discriminating.

Or, it could be that one of the double ratios deviates from unity by a much larger amount than the others, in which case it might be most discriminating even if the R^h's involved are not measured with great precision.

- In Fig. 16, we plot the numerator versus the denominator of the double ratios I) and II), [III) being very like I) due to the correlation between the $R^h_{gg}(\gamma\gamma)$ and $R^h_{gg}(VV)$ values discussed earlier].
- We observe that any one of these double ratios will often, but not always, deviate from unity (the diagonal dashed line in the figure).
- The probability of such deviation increases dramatically if we

require (as apparently preferred by LHC data) $R^h_{gg}(\gamma\gamma) > 1$, see the solid (vs. open) symbols of Fig. 16.

- This is further elucidated in Fig. 17 where we display the double ratios I) and II) as functions of $R^h_{gg}(\gamma\gamma)$ (left plots).

  For the NMSSM, it seems that the double ratio I) provides the greatest discrimination between degenerate vs. non-degenerate scenarios with values very substantially different from unity (the dashed line) for the majority of the degenerate NMSSM scenarios explored in the earlier section of this talk that have enhanced $\gamma\gamma$ rates.

  Note in particular that I), being sensitive to the $b\bar{b}$ final state, singles out degenerate Higgs scenarios even when one or the other of h_1 or h_2 dominates the $gg \to \gamma\gamma$ rate, see the top right plot of Fig. 17.

  In comparison, double ratio II) is most useful for scenarios with $R^h_{gg}(\gamma\gamma) \sim 1$, as illustrated by the bottom left plot of Fig. 17.

- **Thus, as illustrated by the bottom right plot of Fig. 17, the greatest discriminating power is clearly obtained by measuring both double ratios.**

In fact, a close examination reveals that there are no points for which $both$ double ratios are exactly 1!

Of course, experimental errors may lead to a region containing a certain number of points in which both double ratios are merely consistent with 1 within the errors.

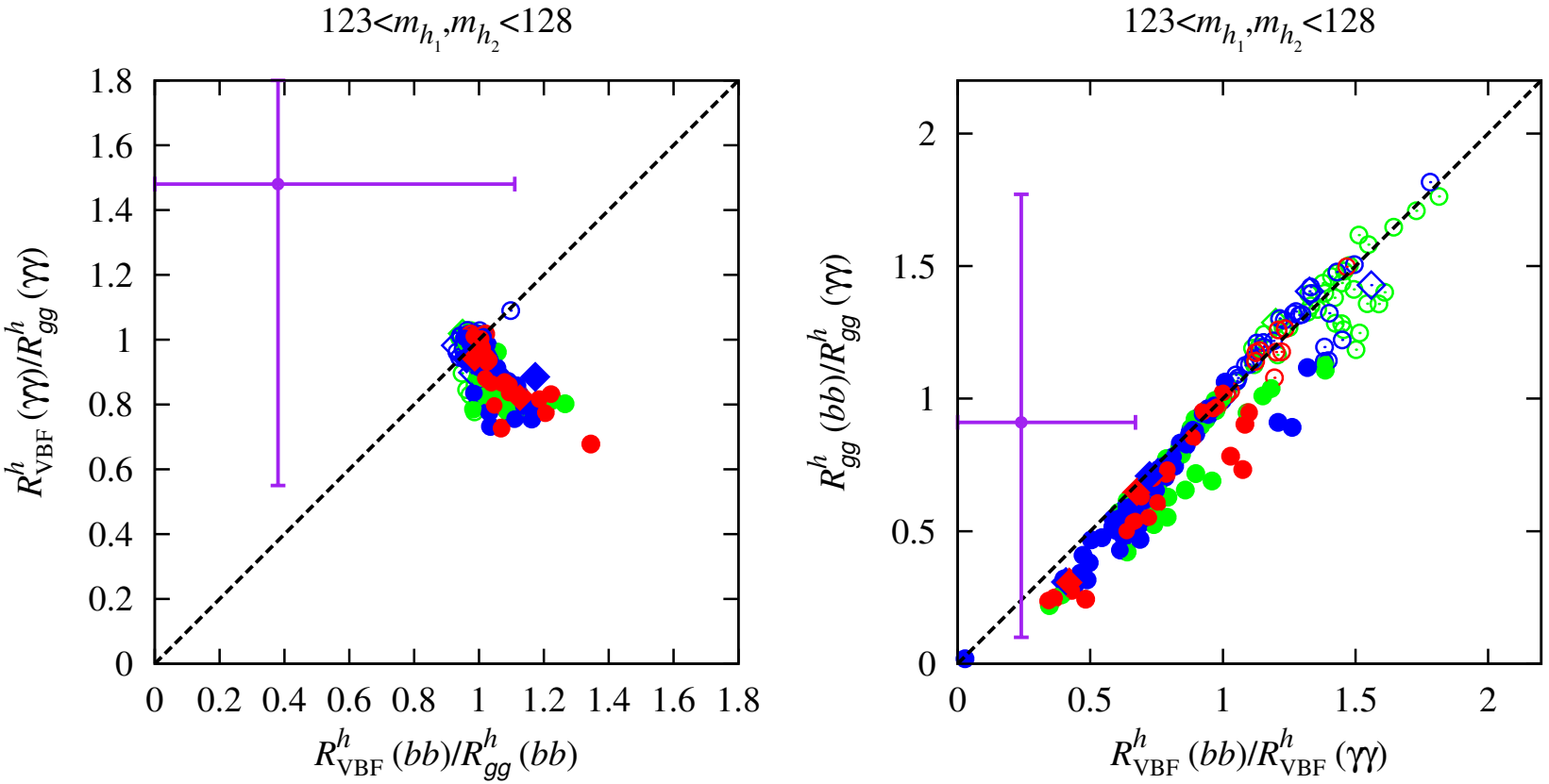

Figure 16: **Comparisons of pairs of event rate ratios that should be equal if only a single Higgs boson is present. The color code is green for points with $2\ \mathrm{GeV} < m_{h_2} - m_{h_1} \leq 3\ \mathrm{GeV}$, blue for $1\ \mathrm{GeV} < m_{h_2} - m_{h_1} \leq 2\ \mathrm{GeV}$, and red for $m_{h_2} - m_{h_1} \leq 1\ \mathrm{GeV}$. Large diamond points have Ωh^2 in the WMAP window of $[0.094, 0.136]$, while circular points have $\Omega h^2 < 0.094$. Solid points are those with $R^h_{gg}(\gamma\gamma) > 1$ and open symbols have $R^h_{gg}(\gamma\gamma) \leq 1$. Current experimental values for the ratios from CMS data along with their 1σ error bars are also shown.**

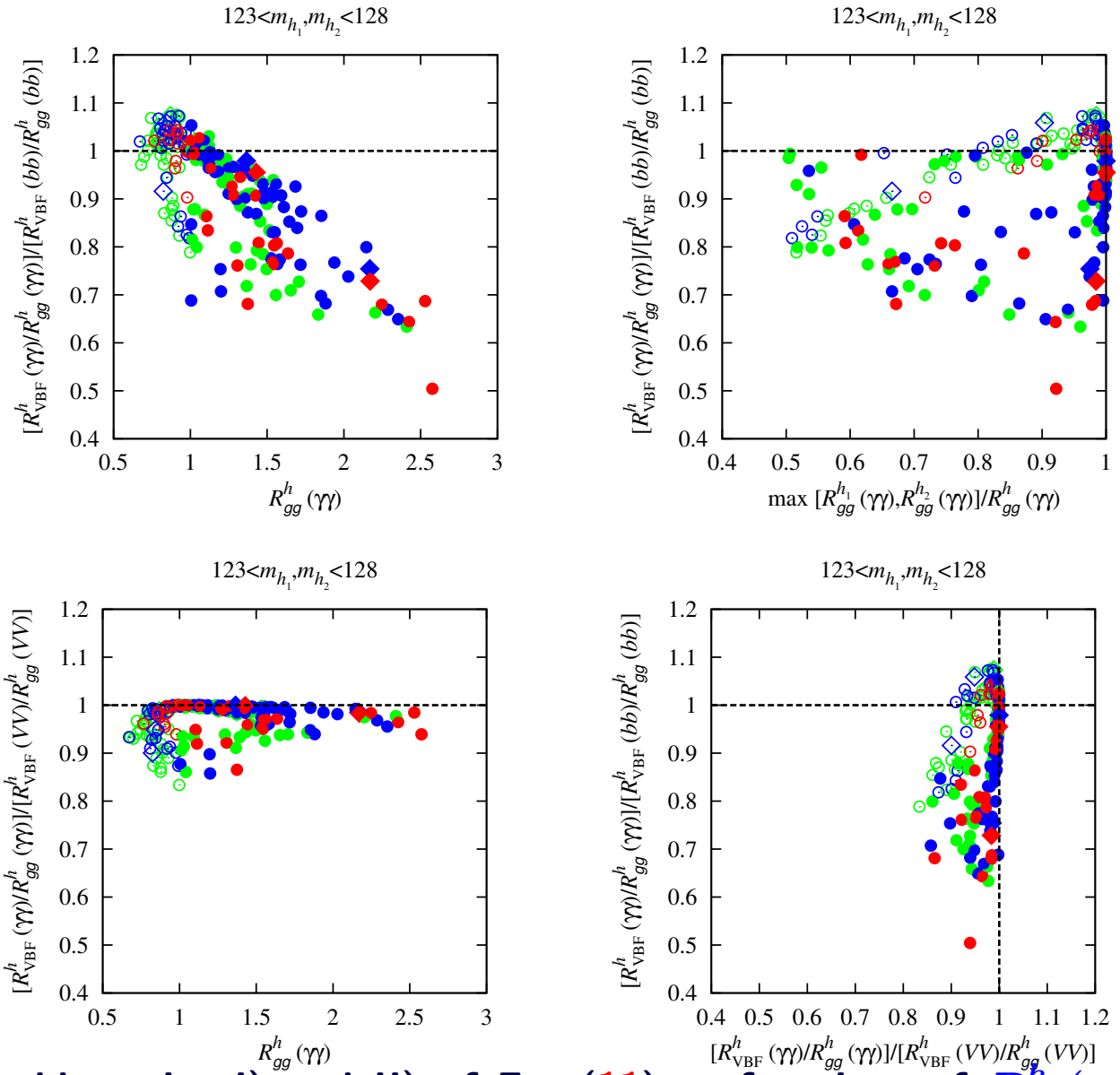

Figure 17: Double ratios I) and II) of Eq. (11) as functions of $R^h_{gg}(\gamma\gamma)$ (on the left). On the right we show (top) double ratio I) vs. $\max\left[R^{h_1}_{gg}(\gamma\gamma), R^{h_2}_{gg}(\gamma\gamma)\right]/R^h_{gg}(\gamma\gamma)$ and (bottom) double ratio I) vs. double ratio II) for the points displayed in Fig. 16. Colors and symbols are the same as in Fig. 16.

- **What does current LHC data say about these various double ratios?**

  The central values and 1σ error bars for the numerator and denominator of double ratios I) and II) obtained from CMS data (CMS-PAS-HIG-12-020) are also shown in Fig. 16.

  Obviously, current statistics are inadequate to discriminate whether or not the double ratios deviate from unity.

  About 100 times increased statistics will be needed. This will not be achieved until the $\sqrt{s} = 14$ TeV run with ≥ 100 fb^{-1} of accumulated luminosity.

  Nonetheless, it is clear that the double-ratio diagnostic tools will ultimately prove viable and perhaps crucial for determining if the ~ 125 GeV Higgs signal is really only due to a single Higgs-like resonance or if two resonances are contributing.

- **Degeneracy has significant probability in model contexts if enhanced $\gamma\gamma$ rates are indeed confirmed at higher statistics.**

The pure 2HDM

- *"Two-Higgs-Doublet Models and Enhanced Rates for a 125 GeV Higgs"* **A. Drozd, B. Grzadkowski, J. F. Gunion and Y. Jiang. arXiv:1211.3580 [hep-ph]**
- **see also,** *"Mass-degenerate Higgs bosons at 125 GeV in the Two-Higgs-Doublet Model"* **P. M. Ferreira, H. E. Haber, R. Santos and J. P. Silva. arXiv:1211.3131 [hep-ph]**
- **There are some differences.**

NMSSM-like degeneracy can be explored in this context also, but no time to discuss.

Conclusions

- It seems likely that the Higgs responsible for EWSB has emerged.
- Perhaps, other Higgs-like objects are emerging.
- Survival of enhanced signals for one or more Higgs boson would be one of the most exciting outcomes of the current LHC run and would guarantee years of theoretical and experimental exploration of BSM models with elementary scalars.
- $>$SM signals would appear to guarantee the importance of a linear collider or LEP3 or muon collider in order to understand fully the responsible BSM physics.
- In any case, the current situation illusrates the fact that we must never assume we have uncovered all the Higgs.

Certainly, I will continue watching and waiting